ICES Journal of Marine Science, 2023, **0**, 1–13
DOI: 10.1093/icesjms/fsad156
Original Article

Quantifying the ability of imaging sonar to identify fish species at a subtropical artificial reef

E. C. P. Sibley [1,2,*], A. S. Madgett [2,3], J. M. Lawrence [4], T. S. Elsdon [5], M. J. Marnane [5], and P. G. Fernandes [4]

[1]School of Biological Sciences, King's College, University of Aberdeen, Aberdeen AB24 3SW, UK
[2]The National Decommissioning Centre, Newburgh, Aberdeenshire AB41 6AA, UK
[3]School of Engineering, University of Aberdeen, Aberdeen AB24 3AA, UK
[4]The Lyell Centre, Heriot-Watt University, Research Avenue South, Edinburgh EH14 4AP, UK
[5]Chevron Technical Centre, Perth, WA 6000, Australia

[*] *Corresponding author:* e-mail: e.sibley.20@abdn.ac.uk.

Imaging sonars (ISs) are high-frequency acoustic devices that are increasingly being used to study fish in marine and freshwater habitats. Acoustic devices are limited in quantifying species richness, and previous attempts to identify fish species using IS have mostly focused on assemblages of low species richness or high morphological diversity. This study aimed to determine the ability of IS for identifying fish species at a subtropical artificial reef off Perth, Western Australia. Several fish traits that could be defined using IS were identified and described for all fish species observed with simultaneous optical footage. These traits were used to create a clustering algorithm to infer the species identity of IS detections of the five most abundant species at the reef. The identities of all fish from two species (*Chromis westaustralis* and *Neatypus obliquus*) were inferred with 100% success, though no individuals from the remaining three species (*Seriola dumerili*, *Coris auricularis,* and *Pempheris klunzingeri*) were correctly identified. An alternative clustering-based approach to categorising fish detected by IS independent of taxonomic inference was also implemented. Overall, this study demonstrates that IS can identify reef fish with variable success, and proposes an alternative method for describing fish assemblages irrespective of species identity.

Keywords: acoustics, artificial reef, classification, clustering, schooling, size, taxonomy.

Introduction

Non-invasive approaches to surveying fish populations can be broadly categorized as acoustic or optic. Optical survey methods (e.g. high-definition video, SCUBA censuses) rely on visual appraisal of fish assemblages. In contrast, acoustic methods quantify fish through the propagation of sound waves in the water column and detection of echoes produced when the sound intercepts an object. Unlike optical methods, acoustics can operate independently of light and visibility, and are therefore the preferred approach to surveying fish in deep water (Giorli and Au, 2017; Giorli *et al.*, 2018), at night (Becker *et al.*, 2013; Jůza *et al.*, 2013), or in turbid water (Moursund *et al.*, 2003; Mueller *et al.*, 2006).

Imaging sonars (also known as acoustic cameras; hereafter termed "ISs") are high-frequency acoustic instruments that generate video-like images of objects (Belcher *et al.*, 2001). ISs are increasingly used in fisheries acoustics due to the greater two dimensional resolution afforded in comparison to lower-frequency echosounders that typically operate at 18-200 kilohertz (kHz; Moursund *et al.*, 2003; Simmonds and MacLennan, 2005; Sibley *et al.*, 2023a), providing detailed images of targets at the cost of shorter detection ranges. Although broadband split-beam echosounders (SBES) have high resolution (Stanton *et al.*, 2010), this is in a single dimension (typically the vertical): unless objects are sufficiently low in density, there may be many objects at the same vertical range within the large horizontal extent of the SBES pulse, which would not allow for targets to be resolved effectively. SBES also have smaller beamwidths compared to the sum of the individual beams in many ISs, which means that, particularly at the short ranges where ISs operate effectively, less of the water is sampled by SBES. At 1.8 megahertz (MHz) and above, objects as small as 1–2 cm can be detected using ISs in two dimensions (Kimball *et al.*, 2010; Dunn *et al.*, 2023). Moreover, ISs have been shown to generate estimates of fish density that are commensurate with alternative survey methods, including mark-recapture (Pipal *et al.*, 2012), gillnetting (Faulkner and Maxwell, 2020), trawling (Rakowitz *et al.*, 2012), and human counts (Holmes *et al.*, 2005; Faulkner and Maxwell, 2020). ISs operating at several frequencies can even outperform traditional optical cameras in quantifying reef fish density (Sibley *et al.*, 2023b). Additionally, the resolution of ISs is high enough that assorted characteristics of fish targets can be observed, including morphological traits (e.g. fins–Langkau *et al.*, 2012; Boulêtreau *et al.*, 2018) and various behaviours, for example, locomotion (Rose *et al.*, 2005; Zhang *et al.*, 2014) and predation (Becker *et al.*, 2011a, 2011b).

However, all acoustic methods are limited in the ability to taxonomically identify fish, principally due to the absence of colour that underpins identification of species using optical methods, but also the high resolution needed to accurately quantify size and describe shape and behaviour. Despite the relatively high frequency of ISs, previous attempts to classify detected fish have achieved variable success and are often only relevant for a specific system, circumstance, or fish

Received: 26 May 2023; **Revised:** 18 August 2023; **Accepted:** 20 September 2023

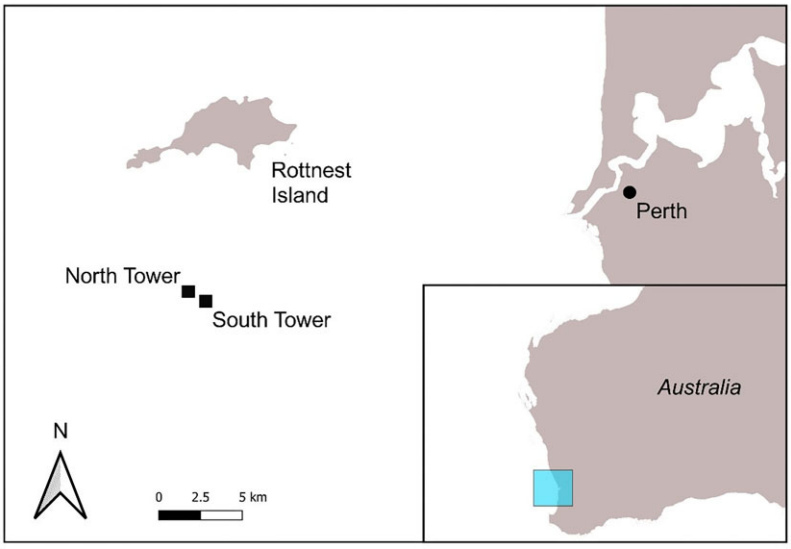

Figure 1. Location of the SRFT, relative to the North Rottnest Fish Tower, Rottnest Island, and Perth. The inset map shows the study region (in by the blue rectangle) relative to the western coast of Australia.

assemblage (see e.g. Rose *et al.*, 2005; Cotter and Polagye, 2020; Artero *et al.*, 2021). As discussed by Grote *et al.* (2014) and Jones *et al.* (2021), successful identification of fish detected by ISs often necessitates conspicuous morphological variation between the ensonified (i.e. acoustically detected) species. Moreover, successful identification is often only achieved for morphologically distinct taxa that are typically at least 20–30 cm in length (Langkau *et al.*, 2012; Jones *et al.*, 2021), reducing the likelihood of identification in fish assemblages comprised of small, morphologically homogeneous fish (e.g. mixed baitfish aggregations—Becker *et al.*, 2011a; Becker and Suthers, 2014).

Traditionally, four characteristics have been used to discriminate fish in manual processing of IS footage: swimming pattern (e.g. Parsons *et al.*, 2014; Keefer *et al.*, 2017), body shape (e.g. Rose *et al.*, 2005; Becker *et al.*, 2011a; Boulêtreau *et al.*, 2018), length (e.g. Magowan *et al.*, 2012; Gurney *et al.*, 2014), and discrete morphological features (Frias-Torres and Luo, 2009; Boulêtreau *et al.*, 2018; Jones *et al.*, 2021). In many circumstances, however, species inferences are made via the collection of alternative evidence that provides information on the composition of the target assemblage, a process sometimes referred to as "ground truth" (McClatchie *et al.*, 2000). Alternative evidence for IS data have been collected using various methods, including extractive techniques such as gillnetting (Lin *et al.*, 2016; Van Hal *et al.*, 2017) and electrofishing (Hughes and Hightower, 2015), and optical instruments (e.g. cameras–Cotter and Polagye, 2020; Lankowicz *et al.*, 2020). However, acquiring alternative evidence is not always possible. For example, ISs have been used extensively in artificial habitats of high structural complexity (e.g. piers - Able *et al.*, 2013; Grothues *et al.*, 2016; Shahrestani *et al.*, 2017) where netting methods are not viable due to entanglement risk. Furthermore, the viability of the method used to gather alternative evidence is contingent on the limitations of that method. For example, if the system is highly turbid and very shallow (e.g. estuaries), both optics (Magowan *et al.*, 2012) and netting (Lankowicz *et al.*, 2020) are not viable. Therefore, definitively quantifying the ability of ISs to classify fish species is imperative, not only to compensate for instances when alternative evidence cannot be collected, but to mitigate the need for alternative methods that can be intrusive, costly, and time-consuming to deploy.

This study aimed to resolve the potential of ISs to classify fish by making taxonomic inferences of the most abundant species ($n = 5$) at a biodiverse sub-tropical artificial reef off Perth, Western Australia. This was achieved through the deployment of ISs operating at two frequencies (0.75 and 3 MHz) and collection of simultaneous high-definition optical footage as alternative evidence. The principal objective of the study was to provide a standardized approach to identifying and classifying fish ensonified by ISs through the quantification and interrogation of fish traits that can be captured by IS at both low (0.75 MHz) and high (3 MHz) frequencies, and that are relevant for all fish assemblages. Moreover, the study aimed to provide an alternative protocol for classifying fish regardless of species identity that can be used to describe ensonified fish assemblages beyond estimations of density. Both objectives were achieved using a cluster-based approach to analyse the fish traits captured by IS that were both categorical and numerical.

Methods

Study site

Simultaneous IS and optical footage was collected from the South Rottnest Fish Tower (SRFT), 27 km off the coast of Perth, Western Australia, at 32° 07'.527 S, 115° 27'.013 E (Figure 1). The SRFT is one of a pair of purpose-built artificial reefs deployed as fish aggregating devices in 2017, standing 12.5 m tall, 10 m long, and 7.8 m wide, and positioned on unconsolidated soft sediment. A further description and a schematic of the SRFT can be found in Sibley *et al.* (2023b). Sampling took place on 28th September 2021 during daylight hours (09:30–13:30). Optical visibility was estimated at 15–25 m throughout the study using the onboard camera of the remotely operated vehicle (ROV; see "Instruments" Section).

Table 1. Species detected using the optic camera at the SRFT ($n = 29$), clustered on maximum size and schooling tendency. The relative abundance of each species is also categorized as rare (<5 individuals), infrequent (5–20 individuals), or common (>20 individuals). ∗ Denotes the five dominant species (in bold) at the SRFT that were carried forward for the species prediction process. † Denotes the medoid species for each cluster.

Cluster 1			Schooling tendency			
Common name	Latin name	Max. size (cm)	Solitary	Pair	Schooling	Abundance
Western Shovelnose Stingaree	*Trygonoptera mucosa*	44.0	✓	✗	✗	Rare
Whitebarred Boxfish†	*Anoplocapros lenticularis*	33.0	✓	✗	✗	Rare
Cluster 2						
Banded Seaperch	*Hypoplectrodes nigroruber*	30.0	✓	✗	✓	Rare
Breaksea Cod	*Epinephelides armatus*	56.0	✓	✗	✓	Rare
Magpie Morwong†	*Goniistius gibbosus*	30.0	✓	✗	✓	Rare
Tarwhine	*Rhabdosargus sarba*	80.0	✓	✗	✓	Infrequent
Cluster 3						
Rough Bullseye*	*Pempheris klunzingeri*	18.0	✗	✗	✓	Common
Splendid Perch	*Callanthias australis*	49.0	✗	✗	✓	Infrequent
Yellowtail Grunter†	*Amniataba caudavittata*	30.0	✗	✗	✓	Rare
Cluster 4						
King George Whiting	*Sillaginodes punctatus*	72.0	✓	✓	✓	Infrequent
Mosaic Leatherjacket	*Eubalichthys mosaicus*	60.0	✓	✓	✓	Rare
Roundface Batfish†	*Platax teira*	70.0	✓	✓	✓	Rare
Skipjack Trevally	*Pseudocaranx wrighti*	70.0	✓	✓	✓	Infrequent
Cluster 5						
Baldchin Groper†	*Choerodon rubescens*	90.0	✓	✓	✓	Rare
Blacktip Trevally	*Caranx heberi*	88.0	✓	✓	✓	Rare
Silver Trevally	*Pseudocaranx georgianus*	94.0	✓	✓	✓	Infrequent
Cluster 6						
Greater Amberjack*	*Seriola dumerili*	190.0	✓	✓	✓	Common
Samsonfish†	*Seriola hippos*	150.0	✓	✓	✓	Infrequent
Cluster 7						
Bluespotted Leatherjacket	*Eubalichthys caeruleoguttatus*	38.0	✓	✓	✓	Infrequent
Moonlighter	*Tilodon sexfasciatus*	40.0	✓	✓	✓	Infrequent
Old Wife	*Enoplosus armatus*	50.0	✓	✓	✓	Rare
Rosy Goatfish	*Parupeneus chrysopleuron*	55.0	✓	✓	✓	Rare
Southern Maori Wrasse†	*Ophthalmolepis lineolata*	40.0	✓	✓	✓	Rare
Western King Wrasse*	*Coris auricularis*	40.0	✓	✓	✓	Common
Cluster 8						
Brokenline Wrasse	*Stethojulis interrupta*	13.0	✓	✓	✓	Rare
Footballer Sweep*	*Neatypus obliquus*	22.0	✓	✓	✓	Common
Redband Wrasse†	*Pseudolabrus biserialis*	17.2	✓	✓	✓	Infrequent
West Australian Puller*	*Chromis westaustralis*	8.5	✓	✓	✓	Common
Western Talma	*Chelmonops curiosus*	26.0	✓	✓	✓	Rare

Instruments

Fish at the SRFT were acoustically detected using two Blueprint Subsea Oculus multibeam ISs (www.blueprintsubsea.com/oculus/oculus-m-series): the M750d (operating at 0.75 MHz, range set to 10 m), and the M3000d (3 MHz, 5 m). The specifications of both ISs are detailed in Table S1. Each IS was interchangeably deployed atop an Oceanbotics SRV-8 ROV (www.oceanbotics.com/srv-8/). Each IS was mounted in the same vertical plane as the onboard camera of the ROV to permit simultaneous capture of IS and optical footage (Figure S1). The camera was situated behind a dome port and recorded video at 1080p (30 fps), with vertical and horizontal viewing angles of 65.4° and 99.1°, respectively. The ROV was tethered to the surface via an umbilical, with an ultra-short baseline (USBL) positioning system used to determine its location. The ROV also housed an altimeter to record depth. The ROV was orientated (pitch and tilt) orthogonally to the SRFT throughout the survey.

Data acquisition and IS trait assignation

IS data and optical footage were collected by piloting the ROV around the periphery of the SRFT at three depth strata: the lower strata (the base of the tower, from the seabed to ∼3 m above the seabed), the upper strata (the top of the tower, between ∼3 and 6 m above the seabed) and the spire (a pyramid of four converging beams projecting from the top of the tower to 12.5 m above the seabed). To acquire the additional evidence needed to resolve the species identity of the ensonified fish (e.g. Becker *et al.*, 2013; Lankowicz *et al.*, 2020), all species observed in the simultaneous optical footage when operating the ISs at each frequency were recorded ($n = 29$, Table 1).

The optical camera footage revealed the fish assemblage of the SRFT to be dominated (i.e. with abundances >20) by five species: greater amberjack (*S. dumerili*), western king wrasse (*C. auricularis*), rough bullseye (*P. klunzingeri*), West Australian puller (*C. westaustralis*), and footballer sweep (*N. obliquus*). To ensure sufficient replication for further analyses, only fish of these species were recorded for IS trait determination (see below). Both the optical and IS footage were reviewed continuously, with observations of these species on the optical footage matched to the simultaneous IS footage to confirm identity (Figure 2). Only fish that were completely in the field of view of both the IS (i.e. not obstructed by the various factors that impact IS fish detection described in Sibley *et al.*, 2023b, including masking from benthic growth and physical habitat

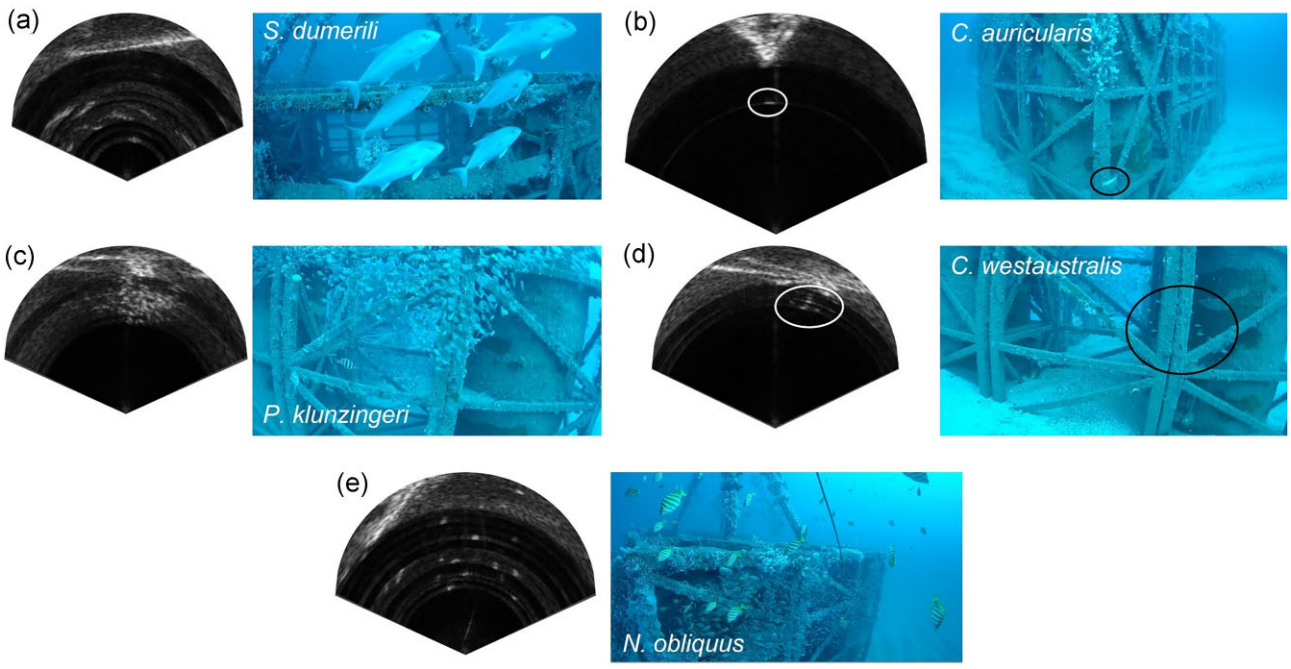

Figure 2. Simultaneous IS and optical still frames of the five most abundant species at the SRFT: (a) a school of greater amberjack (*S. dumerili*); (b) a solitary western king wrasse (*C. auricularis*), circled in white and black on the IS and optic frames respectively; (c) a school of rough bullseye (*P. klunzingeri*); (d) a school of West Australian puller (*C. westaustralis*), circled; and (e) a school of footballer sweep (*N.obliquus*). All IS frames were captured at 0.75 MHz. The ensonified physical structure of the SRFT can be seen in the background of each IS frame as a dense reflective object. The IS frames are cropped from the original display as best to depict each species.

structure ensonification) and the optical camera (i.e. such that species identification was possible) were used ($n = 296$). The sample size for each species comprised the minimum number of each species observed using the optical footage at each IS frequency trial: *S. dumerili*, $n = 24$ (combined n at each frequency = 48); *C. auricularis*, $n = 21$ (42); *P. klunzingeri*, $n = 27$ (54); *C. westaustralis*, $n = 41$ (82); and *N. obliquus*, $n = 35$ (70). IS footage from all sites was inspected and analysed using Oculus Viewpoint software (www.blueprintsubsea.com/oculus/support.php). Optical footage was inspected using RJE SubNav software (v1.2.38; www.oceanbotics.com/sub-nav/).

Fish that were retained for further analyses (i.e. one of the five dominant species listed above) were described using three traits derived from the IS. The traits chosen for this classification were those that could be readily quantified using most IS post processing software, including Oculus Viewpoint, and are applicable to all marine fish assemblages. Three traits were selected: fish size, schooling tendency, and body shape.

Fish size was defined as the total linear body length of the fish in cm, and estimated using the measuring tool on the Oculus Viewpoint software. The continuous IS footage was paused whilst size was measured. Across all frequencies, the minimum size measurable was 5 cm, identified as the minimum length that could be consistently quantified using the measuring tool at the lowest frequency (0.75 MHz). All fish that were the same length or smaller than this minimum measurable size were recorded as 5 cm. Measurements were taken when fish were oriented as close to linear (i.e. not perpendicular relative to the IS beam array) and as conspicuous in the display (i.e. as close to the centre of the beam array) as possible. Only fish within 4 m range were measured as size estimates at long ranges are known to be erroneous due to decreased resolution and greater absorption of sound waves (Burwen *et al.*, 2010; Hightower *et al.*, 2013; Giorli *et al.*, 2018; Daroux *et al.*, 2019). Although Helminen *et al.* (2020) deemed these effects to be negligible within 29 m at 1.1 MHz, the incidence of this range effect is likely greater at the 3 MHz frequency used here.

The schooling tendency of fish detected on the IS was allocated by combining several definitions of fish schooling from previous studies (Pitcher, 2001; Viehman and Zydlewski, 2015; Becker *et al.*, 2016; Van Hal *et al.*, 2017). Fish were ultimately assigned to one of three schooling tendency categories: solitary, paired, or schooling. A solitary fish was alone and not swimming in the same direction as, nor behaving similarly to, nor a similar size to any other fish. Paired fish were two fish swimming in the same direction as, behaving similarly to, and of a similar size to each other. Fish in the schooling category were defined as swimming in the same direction as, behaving similarly to, and of similar size to two or more other fish. Preliminary inspection revealed paired and schooling fish to be in variable proximity to the nearest other fish irrespective of body length. Therefore, proximity in terms of body lengths was not incorporated into the schooling definition. Adjacent frames were used to confirm schooling tendency when it could not be determined from individual still frames.

Body shape was determined through preliminary inspection of the IS footage to be either ellipsoidal or filiform. Ellipsoidal fish tapered from head to tail and were widest near the middle of the body). Filiform fish were eel-like with consistent girth across the length of the body. Targets that are detected by ISs in three-dimensional space are displayed in two dimensions, horizontal, and range (i.e. X and Z; Martignac *et al.*, 2015).

Vertical-dimensional traits, therefore, cannot be observed, so complete profiles of body shape are not possible. Body shape categorization by ISs is very limited, and is further restricted by the lower resolution of ISs than optics. For example, depressiform and compressiform fish cannot be readily distinguished from one another, unless either phenotype is particularly conspicuous (e.g. the expansive compressiform shape of large Mobula rays–McCauley *et al.*, 2014; Artero *et al.*, 2021), or supplemented by other distinguishing morphological traits (e.g. the fencing sword-like tails of Mylobatid rays–Parsons *et al.*, 2017). The majority of both depressiform and compressiform fish, as well as all fusiform fish, therefore fit the definition of ellipsoidal. This leaves filiform fish (e.g. Muraenids, Fistularids) as the only other broad fish morphology that is distinguishable using ISs.

All recordings and trait assignations were made by the same observer (E.C.P. Sibley) to negate potential inter-observer variation (Keefer *et al.*, 2017; Jones *et al.*, 2021). Measured fish were simultaneously tracked using continuous optic footage to mitigate double counting and repeat measurements (e.g. Becker *et al.*, 2016), to minimize the risk of pseudo-replication as experienced in Jones *et al.* (2021). However, repeat measurements of more motile (e.g. footballer sweeps) and densely schooling species (e.g. greater amberjack) that can recurrently move in and out of the frame and are challenging to isolate from conspecifics may still have occurred on occasion (as per the multipass hypothesis of Brehmer *et al.*, 2006), particularly for any fish that followed the ROV (McLean *et al.*, 2020; Wetz *et al.*, 2020).

Clustering and species predictions

The clustering and species prediction processes comprised five stages. Firstly, prior to processing the IS footage, all fish species optically detected at the SRFT were assigned three traits analogous to the IS traits described above (Table 1). Maximum size was sourced from FishBase (www.fishbase.se/search.php, Froese and Pauly, 2023), quantified as standard length for *C. westaustralis*, and total length for the remaining four species. Though mean size was preferred, this was unavailable for most of the species observed at the SRFT. Schooling tendency, allocated as either solitary, paired, or schooling as per the definitions in Section "Data Acquisition and IS trait assignation", was assigned to each species based on deliberations by several of the authors (E.C.P. Sibley, A.S. Madgett, T.S. Elsdon, and M.J. Marnane) with a combined experience in reef fish surveys spanning several decades. Due to a paucity of species-specific knowledge on fish schooling tendency, this trait was assigned at the family level (for example, all members of the family *Pempheridae* were listed as schooling based on the known gregariousness of different species within that family). Previous experiences of stochastic events that trigger schooling behaviours (e.g. predation; see Viscido *et al.*, 2004, 2007) were not considered; schooling tendency was defined based on "normal" behaviour. Body shape (either ellipsoid or filiform) was assigned to each species based on assumptions as to the appearance of each species on an IS display, facilitated by previous studies that describe the appearance of various taxa of diverse morphology (e.g. Parsons *et al.*, 2017; Francisco and Sundberg, 2019; Artero *et al.*, 2021; Jones *et al.*, 2021).

Secondly, all of the 29 fish species optically observed at the SRFT were clustered on these traits. A cluster distance matrix was formulated using Gower's distance, which accommodates variables of mixed types (Gower, 1971). All fish species were ellipsoid, so body shape was dropped as a variable in the distance matrix formulation. Maximum length was weighted double relative to the remaining variables. The stochasticity and overlap in schooling tendencies among the species observed meant schooling tendency was likely less important than maximum size in the definition of the clusters, a continuous variable that was substantially more effective in discretizing species (see Kaufman and Rousseeuw, 2009). The optimum number of clusters was determined using partitioning around medoids (PAMs) based on the Gower's distance calculation, and silhouette width (SW) calculated for 2–20 clusters. Using the Gower's distance calculation, PAM aggregates observations based on similarity, by first identifying representative observations (termed "medoids"), then assigning similar observations to each medoid to create clusters. The number of clusters that best represents the data is determined using SW, a measure of similarity between pairs of observations relative to both other observations in the same cluster, and observations in the nearest neighbouring cluster. Further description of PAM and SW use in cluster determination can be found in the Methods of Lawrence and Fernandes (2022).

Thirdly, the PAM algorithm was customised to specify the number of clusters (k) with the highest SW (Batool and Hennig, 2021).

Fourthly, to predict the species identity of the fish observed on the ISs at each frequency (as defined by the traits listed in Section "Data Acquisition and IS Trait Assignation" with species identity confirmed by simultaneous optics), all fish detected on the IS were assigned to one of the clusters defined in stage 2. The schooling tendency of the ensonified fish was matched against the schooling tendencies of each cluster medoid. Clusters with medoids that did not have a matching schooling tendency were excluded. Conjunctively, the size of the ensonified fish was compared to the mean average of the maximum size of all fish species in each cluster (hereafter termed "mean maximum size"), and assigned to the cluster with the closest value. Successful predictions occurred when the assigned cluster contained the species of fish that was identified to be the ensonified fish using the optics. For example, if an ensonified fish was predicted to belong to a cluster containing *C. westaustralis* and the optics confirmed that the fish was indeed *C. westaustralis*, the prediction would be successful.

Fifthly, following the clustering process for species assignment predictions, all fish observed on the IS display underwent the same clustering procedure described in stage 2 in order to classify ensonified fish independent of species identity. Again, all fish observed were ellipsoid, so body shape was dropped. Size was again double weighted relative to the schooling tendency categories. The clustering procedure was identical to the above, except the PAM algorithm was constructed on four clusters. All clustering was done in R (R Core Team, 2013). Distance matrices and PAM algorithms were formulated using the "daisy" and "pam" functions, respectively, in the package "cluster" (Maechler *et al.*, 2012).

Results

For clustering of the 29 species observed at the SRFT, SW was highest at $k = 8$ (SW = 0.69). The resulting PAM algorithm was formulated on eight clusters; although there was high overlap in the mean maximum size of most clusters, vari-

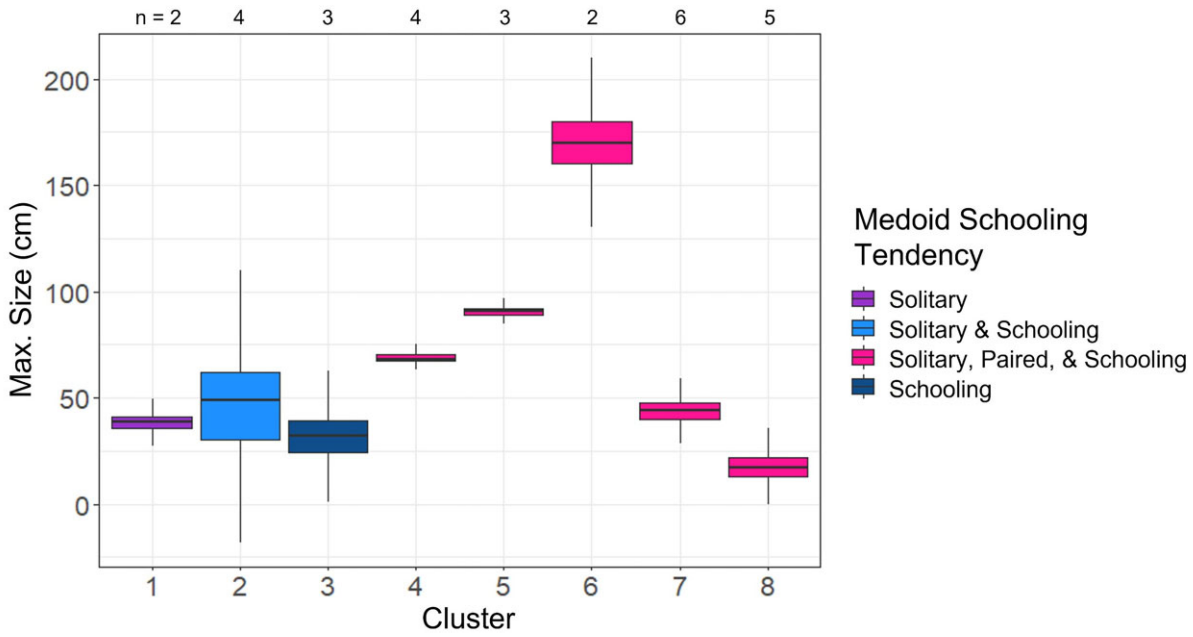

Figure 3. Boxplots showing the distribution of maximum size per cluster, where the horizontal black lines designate the mean maximum size, the whiskers represent 1.5 times the interquartile range above and below the third and first quartile, respectively, and the colour designates the schooling tendency of the medoid species of each cluster. The number of species in each cluster is denoted above each box.

ation in schooling tendency allowed for the distinction of the eight clusters (Figure 3). Predictions for both *C. westaustralis* and *N. obliquus* were both 100% successful across both frequencies (indicated by the doughnut charts in Figure 4d and e); all individuals observed on the ISs from both species were allocated to a cluster containing five species (including *C. westaustralis* and *N. obliquus*), each exhibiting all three schooling tendencies. The mean maximum size of this cluster was 17.3 cm. Success rates for *S. dumerili*, *C. auricularis*, and *P. klunzingeri* were all zero for both frequencies (i.e. no individuals from these species observed on the ISs were allocated to the cluster that contained that species, as shown by the doughnut charts in Figure 4a–c).

Investigation of the length distributions for each of the five species that underwent the prediction process generally demonstrated that fish recorded on the ISs were markedly smaller than the maximum known size for each species (as shown by the histograms in Figure 4), except for *C. westaustralis* whose size ranged from 5 to 18 cm, despite a maximum known size of 8.5 cm (Figure 4e). The observed schooling tendencies of ensonified fish were broadly commensurate with the expected schooling tendencies of their respective species (Table 1, Figure 4). Only *P. klunzingeri* was not listed as practicing all three schooling tendencies, instead described as exclusively schooling species. Solitary individuals comprised 3.7 and 14.8% of *P. klunzingeri* observations at 0.75 and 3 MHz, respectively.

All fish observed on the ISs ($n = 296$) were clustered via PAM at $k = 4$ (SW = 0.87). Because there was no difference in prediction success between 0.75 and 3 MHz (evidencing no difference in the ability to discriminate individual species), nor any conspicuous difference in recorded lengths for each species per frequency, all fish recorded at both frequencies were clustered together. The resulting clusters (hereafter termed imaging sonar groups, ISGs) each contained fish displaying only one schooling tendency. Based on this and the sizes of the constituent fish, ISGs were annotated as follows: ISG 1 = medium-sized solitary fish ($n = 132$); 2 = large schooling fish ($n = 42$); 3 = medium-sized paired fish ($n = 26$); and 4 = small schooling fish ($n = 96$). The size distribution, schooling tendencies, and species composition of each cluster are displayed in Figure 5.

Discussion

Previous investigations into the capacity of ISs to identify fish species have been predominantly based on the detection and discrimination of conspicuous morphological features that distinguish species (e.g. Langkau *et al.*, 2012; Boulêtreau *et al.*, 2018; Jones *et al.*, 2021). However, these approaches have achieved variable success and have generally only been implemented on assemblages containing just a handful of different species (Langkau *et al.*, 2012). This study advances on prior investigations by using two traits, body size and schooling tendency, to categorize and cluster fish detected by IS at a species rich artificial reef off the coast of Western Australia, achieving variable success in the identification of the five most abundant species at the reef (observed using simultaneous optical footage). The systematic approach to species classification presented here can be applied to all fish communities in all ecosystems and contexts, based on the clustering of traits that can be quantified by ISs for all fish species. In addition, a method of classifying ensonified fish that is independent of species identity was explored, for use when the collection of alternative evidence (e.g. optical camera footage) to inform species composition is not possible.

Fish clustering

The two most abundant species, West Australian puller (*C. westaustralis*) and footballer sweep (*N. obliquus*), were both allocated to their corresponding cluster with 100% accuracy at both frequencies. Therefore, it was inferred that all

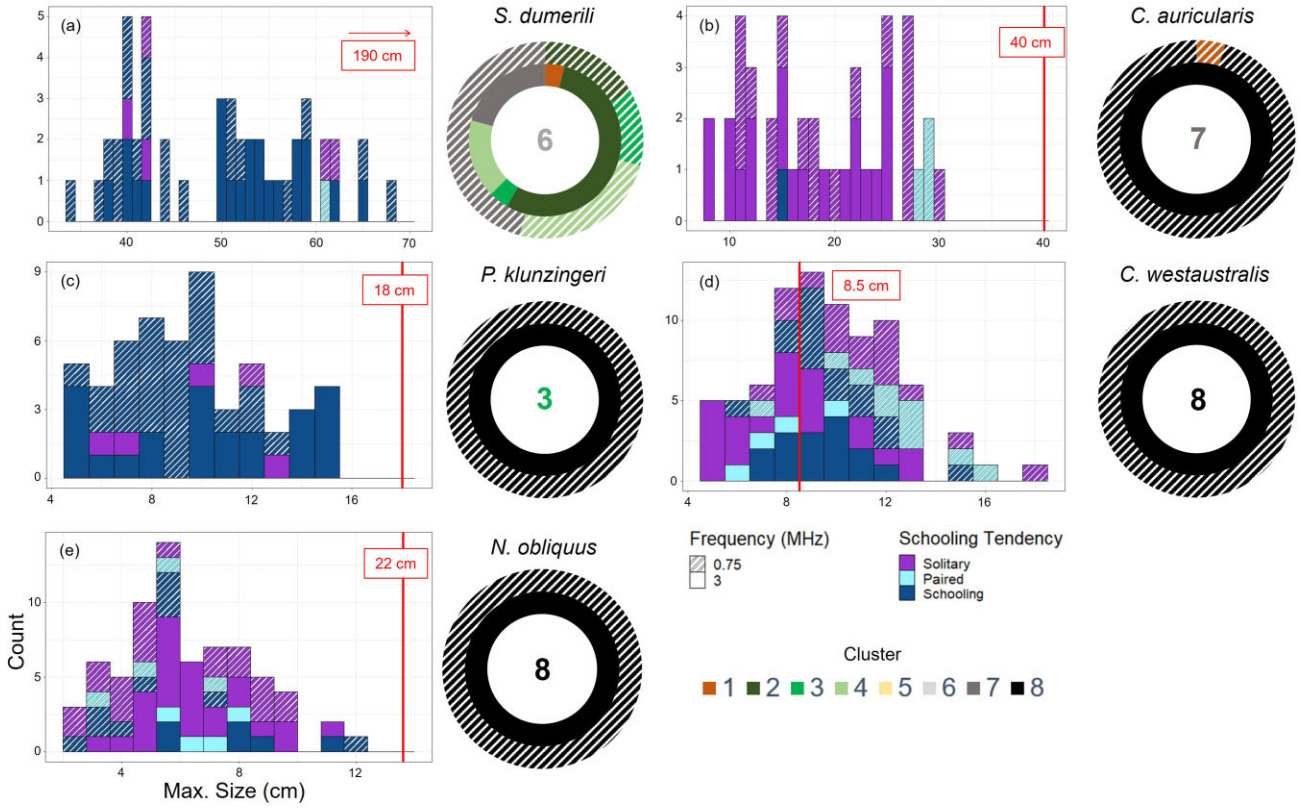

Figure 4. Counts, size distributions, and schooling tendencies of the five most abundant fish species surveyed at both frequencies at the SRFT: (a) greater amberjack (*S. dumerili*), (b) western king wrasse (*C. auricularis*), (c) rough bullseye (*P. klunzingeri*), (d) West Australian puller (*C. westaustralis*), and (e) footballer sweep (*N. obliquus*). Presented on each histogram are the maximum known sizes (red line) of each species derived from FishBase (Froese and Pauly, 2023). Adjacent doughnut charts show the proportions of individuals from each species that were recorded on the IS assigned to the eight clusters presented in Figure 1 based on their size and schooling tendency, with the number in the middle of each chart indicating the cluster to which the corresponding species was allocated. The success of the prediction process is thereby represented in these charts. For example, all *C. westaustralis* and *N. obliquus* individuals were allocated to cluster 8 across both frequencies, the same cluster to which each species was assigned in Table 1. Prediction success was therefore 100% for both of these species at both frequencies. Conversely, all *C. auricularis* individuals were allocated to either cluster 1 or 8, yet *C. auricularis* was assigned to cluster 7. Prediction success was therefore 0% at both frequencies. Shading in the doughnut charts indicates the frequency of the IS used, with hashed areas representing 0.75 MHz, and filled areas representing 3 MHz.

individuals from these species were one of five species (i.e. the number of species in the corresponding cluster for each species; Table 1) as opposed to one of 29 species (the total number of species identified using simultaneous optics at the SRFT). Key to this classification success were the ensonified fish displaying schooling tendencies that reflected the tendencies of their corresponding families, and the length distributions of the ensonified fish being consistent with the maximum known sizes of each species. Notably, the published maximum size of *C. westaustralis* was smaller (8.5 cm) than the largest *C. westaustralis* recorded here (18 cm). This could be a product of length overestimation of smaller fish using IS reported from previous studies (Hightower *et al.*, 2013; Cook *et al.*, 2019; Daroux *et al.*, 2019; Helminen *et al.*, 2020). However, rough bullseye (*P. klunzingeri*) exhibited a size distribution similar to *C. westaustralis* whilst not exceeding the maximum known size for the species. Therefore, it is likely that the maximum size of *C. westaustralis* is much larger than previously reported, instead of the large sizes reported here being a product of measurement error (see Section "Instrumental effects"). Ultimately, this discrepancy did not impact the successful prediction of all *C. westaustralis* individuals, particularly because the other four species in the cluster that contained *C. westaustralis* were all larger, increasing the mean maximum size of the cluster to one at the scale of the larger *C. westaustralis* individuals detected.

Conversely, no individuals of greater amberjack (*S. dumerili*), *P. klunzingeri*, and western king wrasse (*C. auricularis*) were inferred successfully. Although these species exhibited schooling tendencies that generally agreed with their family-level schooling behaviours, their size distributions were smaller than the known maximum sizes for each species. This was particularly apparent for *S. dumerili*: the largest individual recorded was 122 cm smaller than the known maximum size for the species, and amberjacks were instead assigned to several clusters of mean maximum sizes that were more commensurate with the size distribution quantified. The magnitude of the difference between the known maximum size and the recorded size distribution suggests that the *S. dumerili* ensonified here are of an earlier life stage than mature amberjack that would otherwise be closer in size to the known maximum size. Additionally, the majority of ensonified *S. dumerili* exhibited schooling behaviour; as *S. dumerili* mature from juveniles to adolescents, schooling behaviour typically onsets (Miki *et al.*, 2011). Also, the *S. dumerili* observed on the optical camera did not possess the vertical bars along the body that are characteristic of juveniles. These observations in combination imply that the *S. dumerili* around the SRFT are ado-

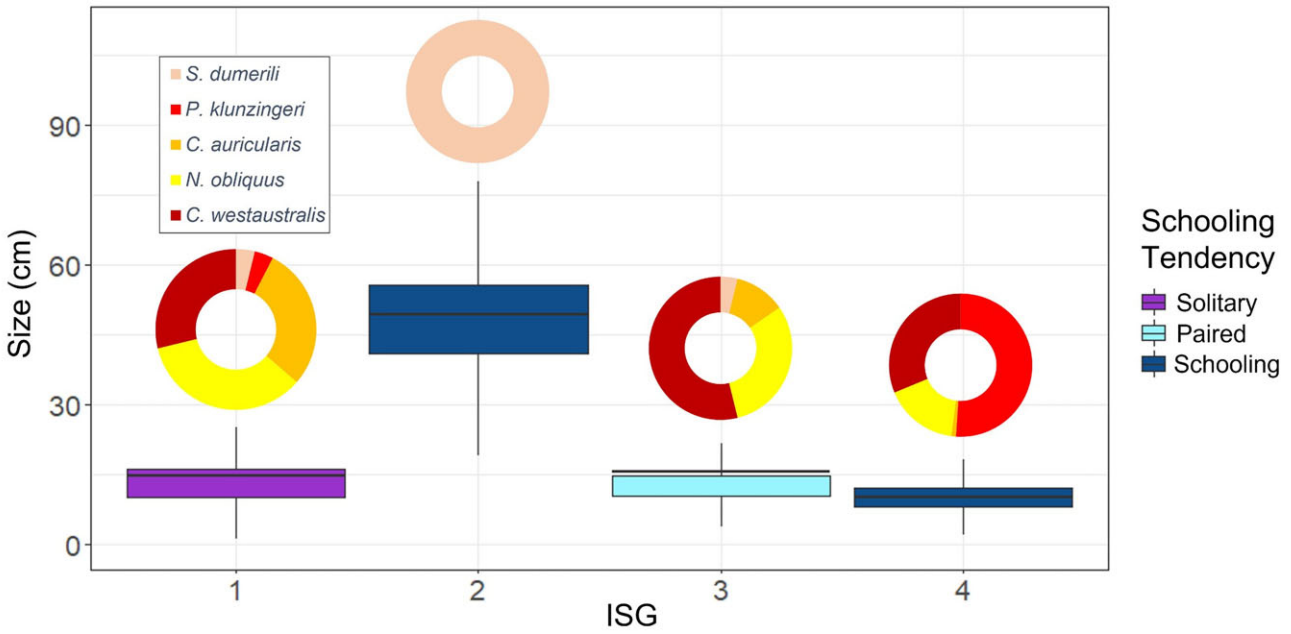

Figure 5. Size distributions (including mean size indicated by the black horizontal line, and whiskers representing 1.5 times the interquartile range above and below the third and first quartile, respectively), for each of the four ISGs as derived from the clustering of the five most abundant species at the SRFT, pooled across both frequencies. All ISGs comprised fish that displayed either a solitary, paired, or schooling tendency, as represented by the colours of each box. Also presented are doughnut charts of the proportional abundance of each species within each ISG.

lescents. Therefore, this study demonstrates the importance of the SRFT in the development of *S. dumerili*, further reinforcing the role of artificial structures in carangid reproduction and recruitment (Folpp *et al.*, 2013; Madgett *et al.*, 2022).

Markedly, this study mirrors previous reports concerning the issue of using size to discriminate fish species ensonified by ISs. In Grabowski *et al.* (2012), the application of discrete size criteria to identify individual species resulted in the frequent misclassification of juveniles whose size distribution did not agree with that of adults from their corresponding species. This parallels the misclassification of *S. dumerili* detected in this study, despite size being measured on a continuous scale. The issue of cohort size variation was mitigated in Crossman *et al.* (2011), where IS estimates of sturgeon size were compared with known length-at-age data to discriminate between individuals from different cohorts, albeit in a monospecific context. Here, this study considers that the number of successful species inferences made for *S. dumerili*, *P. klunzingeri*, and *C. auricularis* would likely be far higher if the mean size of each species (*in lieu* of cohort-specific size data) had been used in the clustering process instead of the maximum size. However, such data were scarce for the majority of observed species, due to the need for the sampling of a large number of individuals, instead of using anecdotal and opportunistic reporting of particularly large individuals from which maximum size is defined. Most of the species at the SRFT are not common fisheries targets, so length estimates from catch data are not available. Additionally, although the common (i.e. mean) size of *S. dumerili* is published on FishBase as 100 cm, this is still 32 cm greater than the largest individual measured here. Therefore, use of mean size would likely result in similar outcomes for *S. dumerili* classification as the use of maximum size here.

The taxonomic inferences made in this study would also be further discretized, and therefore likely improved, through dedicated profiling of schooling tendencies at the species or genus level. Given the paucity of species-specific schooling information for reef fish, this study allocated schooling tendencies to the 29 species at the SRFT at the family level, resulting in high overlap between species. For example, four of the five most abundant species were annotated as displaying solitary, paired, and schooling behaviour. Refining the schooling tendencies of these species at a higher taxonomic resolution would likely partition each species further during clustering, increasing the resolution of taxonomic inferences. Furthermore, schooling behaviours in many fish species can be highly variable, and a product of both biotic and abiotic influences (Viscido *et al.*, 2004, 2007; Rieucau *et al.*, 2015). Stochastic schooling behaviours that are not representative of general schooling tendency may have been ensonified in this study, undermining taxonomic inferences. However, the cumulative impact of this is likely to be minimal, given the overlap in schooling tendencies across the five focal species. Furthermore, most *P. klunzingeri* individuals showed exclusively schooling behaviour, agreeing with our prior categorization of schooling tendency for the family *Pempheridae*. Regardless, no successful species inference for any *P. klunzingeri* individual was made, suggesting the categorical variable of schooling tendency is less important than the continuous variable of size for accurate taxonomic inferences, despite the species medoid of the cluster containing *P. klunzingeri* annotated to also show schooling behaviour only.

The mixed success of taxonomic inferences from IS detections reported here prompted alternative consideration as to how to classify ensonified fish, not least to provide fish assemblage descriptions beyond density estimates. This study clustered all fish detected by the ISs, defined by size and schooling tendency, into four ISGs. Interestingly, each ISG was characterised by one particular schooling tendency that generally corresponded to the schooling tendencies of the composite

species (made available by the use of simultaneous optical footage). Most conspicuously, fish from ISG 2 were exclusively schooling, and were all identified to be *S. dumerili* using the simultaneous optical data. Given that this study annotated *S. dumerili* as exhibiting solitary, paired, and schooling tendencies, the exclusively schooling composition of ISG 2 confirmed that all constituent fish were schooling *S. dumerili*. Moreover, the majority of *P. klunzingeri* (exclusively schooling) were found in ISG 4, which was also categorized as a distinctly schooling group.

ISGs were also defined by an apparent dichotomy in size distribution; the fish in ISG 2 had a much larger mean size than fish from ISGs 1, 3, and 4, which in turn were similar in mean size to each other. This is reflected by the species composition of each ISG, with the larger mean size for ISG 2 attributable to the exclusive composition of *S. dumerili* that are much larger than the other four species. Combined, the schooling tendencies and size distributions of fish in each ISG allowed this study to describe the SRFT assemblage independent of taxonomic inference, albeit this was still made possible by the collection of optical alternative evidence. Using ISGs only, the SRFT assemblage comprised: medium-sized solitary fish ($n = 132$), large schooling fish ($n = 42$), medium-sized paired fish ($n = 26$); and small schooling fish ($n = 96$). This annotation provides significantly more insight into the dynamics of the assemblage than basic density estimates. This study advises the adoption of this classification approach in future studies where the collection of alternative evidence to infer species composition is not viable. In addition to body shape for morphologically diverse assemblages, the approach can be refined by including other traits that are quantifiable on ISs, like schooling density (see Rieucau *et al.*, 2015), that are pertinent in particular contexts, such as when examining predator-prey interactions (e.g. Becker *et al.*, 2011a, 2011b; Boulêtreau *et al.*, 2018).

Instrumental effects

The taxonomic inferences made on the SRFT fish assemblage were inherently relative to the capacity of ISs for detecting and measuring fish, as well as observing fish behaviour. In particular, this study emphasises that measurements of fish size using IS are relative and not absolute (Artero *et al.*, 2021), especially given that no alternative methods to measure fish size were applied that can quantify measurement error (e.g. Lin *et al.*, 2016; Kerschbaumer *et al.*, 2020; Artero *et al.*, 2021; Bennett *et al.*, 2021). Nevertheless, to reduce the incidence of measurement error, only fish within a relatively short range (4 m) were included in this study.

The need for relative appraisal and interpretation of fish sizes stems from the assorted drivers of erroneous fish measurements using ISs, as reported by numerous previous studies that have ensonified and measured fish of known size. These drivers often concern characteristics of the fish themselves, including aspects of fish locomotion (such as swimming style, speed, and behaviour–Burwen *et al.*, 2010; Hightower *et al.*, 2013; Zhang *et al.*, 2014; Keefer *et al.*, 2017; Egg *et al.*, 2018; Cook *et al.*, 2019), fish orientation relative to the IS (specifically the incident angle of the fish, the distance of the fish from the IS, and the position of the fish in the beam array–Tušer *et al.*, 2014; Egg *et al.*, 2018; Giorli *et al.*, 2018; Cook *et al.*, 2019), and morphological differences between fish (e.g. length, girth, body shape, and the focal body parts used in measurement–Burwen *et al.*, 2010; Hightower *et al.*, 2013; Tušer *et al.*, 2014; Cook *et al.*, 2019; Daroux *et al.*, 2019; Helminen *et al.*, 2020; Lagarde *et al.*, 2020). Correction factors for erroneous IS size estimates under these various circumstances are imperative, as inaccurate measurements pose broader connotations for ecological observations and fisheries management, especially when accurate biomass estimates are necessary.

IS specifications can also influence measurement accuracy, with the frequency used being particularly critical. Lower frequencies provide greater range at the cost of resolution, such that targets appear less detailed on the IS display. Given that length measurements are typically made in data post-processing, this means that targets ensonified at lower frequencies are measured with reduced accuracy compared to targets ensonified at higher frequencies (Martignac *et al.*, 2015; Wei *et al.*, 2022). However, there appeared to be no marked differences in the lengths of fish of each species between the low (0.75 MHz) and high (3 MHz) frequencies used in this study, suggesting differences in resolution do not generate conspicuously erroneous size measurements at the scale of the fish assemblage surveyed here. Despite this, the minimum measurable size was 5 cm at 0.75 MHz, so fish below this size (likely including smaller *C. westaustralis* and *P. klunzingeri*) were not consistently detectable, hence their identity could not be inferred. Additionally, the resolution afforded at 3 MHz was still not sufficient to delineate small fish in close proximity to one another (e.g. densely schooling *P. klunzingeri*), a problem that is widely reported in other IS studies of fish communities (Becker *et al.*, 2011a, 2011b, 2016; Becker and Suthers, 2014; Van Hal *et al.*, 2017). Even at high frequencies, the lower resolution of IS relative to optics means quantification of length metrics other than total length that require accurate discrimination of certain features (e.g. fork length) is very challenging, unless those features are conspicuous at the frequencies applied As such, total length ought to be implemented as the standard measurement for fish when using IS, though future studies may look to investigate the feasibility of quantifying alternative length metrics, especially relative to alternative methods (e.g. stereo-video; Harvey *et al.*, 2002).

The manner of data processing can also influence measurement accuracy, with manual length measurement accuracy reported to be contingent on the experience of the observer in identifying fish, particularly in their discrimination from background objects (e.g. non-fish targets, substrate–Viehman and Zydlewski, 2015; Capoccioni *et al.*, 2019; Helminen and Linnansaari, 2021), and instrumental artefacts like side-lobe interference and geometric scattering (Hightower *et al.*, 2013; Cotter and Polagye, 2020). The observer in this study (E.C.P.S.) is experienced in both the identification and measurement of fish using ISs, hence post-processing effects on length measurement accuracy here are likely negligible, if not absent. Ultimately, identifying and quantifying various drivers of fish measurement error using ISs were beyond the scope of this study. The absence of a standardized calibration technique for ISs that can mediate the various causes of erroneous measurements means length estimates cannot be considered absolute (Martignac *et al.*, 2015; Artero *et al.*, 2021).

Finally, the compression of IS data from three-dimensional detections to two dimensions for display results in the loss of details that exist in the Y dimension (Martignac *et al.*,

2015). Although this could impact length measurements and obscure schooling behaviours, the major consequence of target compression in this study was the loss of body shape detail. Subsequently, and despite the high morphological variation of reef fish (Claverie and Wainwright, 2014), only two body shapes (ellipsoid and filiform) were identifiable using ISs. All detected fish from the five focal species were ellipsoid in body shape, such that taxonomic inferences could not be further refined by this characteristic. The increasing application of post-processing software that reconstructs IS data in three-dimensions (Jing *et al.*, 2018), alongside the continued development of three-dimensional ISs (Lagudi *et al.*, 2016), will certainly allow future studies to gauge fish characteristics in greater dimensional detail, potentially increasing the accuracy of taxonomic inferences. Comparably, ISs can be rotated at regular intervals to facilitate size estimates in both lengthward and width-ward dimensions, provided target fish occupy the same position for sufficient lengths of time (Boswell *et al.*, 2019).

Conclusion

This study demonstrated that the species identity of two of the five most abundant fish species at a subtropical artificial reef in Western Australia could be inferred using IS at both low (0.75) and high frequency (3 MHz). However, this study failed to identify any individuals from the remaining three focal species at either frequency. Overall, this investigation concludes that IS can be highly effective at making taxonomic inferences for some fish, but not for others. Through the trait assignation and clustering protocol applied here, this discrepancy appeared to be driven by differences in IS traits between species, in particular fish size, which varies naturally across life history stages. For example, all greater amberjack (*S. dumerili*) detected and measured using IS were markedly smaller than the known maximum size of that species. Accordingly, the amberjacks quantified by IS were assigned to different clusters than the one to which *S. dumerili* was allocated in the primary stage of clustering. Conversely, the size ranges of West Australian puller (*C. westaustralis*) and footballer sweep (*N. obliquus*) were both broadly commensurate with their respective maximum sizes, underpinning a 100% success rate in taxonomic inferences for both species. The variable success of species identification achieved in this study prompted alternative consideration as to effectively classifying fish detected by IS. Through another clustering process, this was achieved by partitioning ensonified fish into one of four distinct clusters termed ISGs, encompassing a range of sizes and schooling tendencies. This study recommends implementing ISGs for future studies of diverse fish assemblages using IS to categorize fish, analogous to low-order taxonomic and functional classifications in optical surveys of fish.

As ISs become more advanced, including the three-dimensional reconstruction of IS footage that can more effectively define morphological characteristics, taxonomic inferences will no doubt become more successful than those achieved here. Nevertheless, a standardized approach for fish classification from IS that works at both low and high frequencies can categorize fish assemblages using characteristics other than species identity. In particular, dedicated investigation of the size distributions, body shapes, and schooling tendencies of different fish species will likely improve the classification approach implemented in this study. Continued profiling and classification of fish assemblages that are diverse in both species richness and morphology, coupled with further interrogation of the traits quantifiable using high-frequency acoustics that can be used to discriminate different fish species, will likely improve the capacity of ISs to provide high-resolution insight into fish communities where optical instruments are not operable.

Acknowledgements

We acknowledge Kevin Holden from DeepVision Subsea, Ben Saunders, Euan Harvey, and Iain Parnum for the collection of video and acoustic imagery. We thank Tony Scarangella for the provision and skippering of the research vessel. We thank Michael Jech and Alejandro Ariza for their provisional comments on the manuscript.

Supplementary data

Supplementary material is available at the *ICESJMS* online version of the manuscript.

Conflict of interest

The authors declare that they have no known conflict financial interests or personal relationships that could have appeared to influence the work reported in this paper. M. J. Marnane and T. S. Elsdon work for Chevron and are interested in understanding the potential ecological and socio-economic value of artificial structures in the marine environment. All the views expressed within the paper are those of the authors and have been uninfluenced by their affiliations.

Funding

This research project was funded by Chevron through a research grant to Curtin University under the Western Australian Energy Research Alliance (AES 17-P2TD-151-A1) and its Anchor Partnership with the UK National Decommissioning Centre. We also acknowledge in-kind support from Net Zero Technology Centre and the University of Aberdeen through their partnership in the UK National Decommissioning Centre.

Ethics statement

The animal study for the collection of field data was reviewed and approved by the Curtin University Animal Ethics Committee (ARE 2021 18).

Data availability

Data will be shared on reasonable request to the corresponding author.

Author contributions

Edward C.P. Sibley conceptualisation, data curation, formal analysis, investigation, methodology, visualisation, writing—original draft, writing—review & editing. **Alethea S. Madgett** project administration, supervision, writing—review & editing. **J. M. Lawrence** formal analysis, investigation, methodology. **Travis S. Elsdon** conceptualisation, funding acquisi-

tion, formal analysis, methodology, project administration, resources, supervision, writing—review & editing. **Michael J. Marnane** conceptualisation, funding acquisition, methodology, project administration, resources, supervision, writing—review & editing. **Paul G. Fernandes** conceptualisation, formal analysis, methodology, project administration, supervision, visualisation, writing—review & editing.

References

Able, K. W., Grothues, T. M., and Kemp, I. M. 2013. Fine-scale distribution of pelagic fishes relative to a large urban pier. Marine Ecology Progress Series, 476: 185–198.

Artero, C., Marchetti, S., Bauer, E., Viala, C., Noel, C., Koenig, C. C., Berzins, R *et al.* 2021. High-resolution acoustic cameras provide direct and efficient assessments of large demersal fish populations in extremely turbid waters. Applied Sciences, 11: 1899.

Batool, F., and Hennig, C. 2021. Clustering with the average silhouette width. Computational Statistics & Data Analysis, 158, pp. 107190. Elsevier.

Becker, A., Whitfield, A., Cowley, P., Järnegren, J., and Næsje, T. 2011a. An assessment of the size structure, distribution and behaviour of fish populations within a temporarily closed estuary using dual frequency identification sonar (DIDSON). Journal of Fish Biology, 79: 761–775.

Becker, A., Cowley, P. D., Whitfield, A. K., Järnegren, J., and Næsje, T. F. 2011b. Diel fish movements in the littoral zone of a temporarily closed South African estuary. Journal of Experimental Marine Biology and Ecology, 406: 63–70.

Becker, A., Holland, M., Smith, J. A., and Suthers, I. M. 2016. Fish movement through an estuary mouth is related to tidal flow. Estuaries and Coasts, 39: 1199–1207.

Becker, A., and Suthers, I. M. 2014. Predator driven diel variation in abundance and behaviour of fish in deep and shallow habitats of an estuary. Estuarine, Coastal and Shelf Science, 144: 82–88.

Becker, A., Whitfield, A. K., Cowley, P. D., Järnegren, J., and Næsje, T. F. 2013. Potential effects of artificial light associated with anthropogenic infrastructure on the abundance and foraging behaviour of estuary-associated fishes. Journal of Applied Ecology, 50: 43–50.

Belcher, E., Matsuyama, B., and Trimble, G. 2001. Object identification with acoustic lenses. In MTS/IEEE Oceans 2001. An Ocean Odyssey. Conference Proceedings (IEEE Cat. No. 01CH37295), pp. 6–11. Honolulu, HI.

Bennett, M. A., Becker, A., Gaston, T., and Taylor, M. D. 2021. Connectivity of large-bodied fish with a recovering estuarine tidal marsh, revealed using an imaging sonar. Estuaries and Coasts, 44: 1579–1587.

Boswell, K. M., Kimball, M. E., Rieucau, G., Martin, J. G., Jacques, D. A., Correa, D., and Allen, D. M. 2019. Tidal stage mediates periodic asynchrony between predator and prey nekton in salt marsh creeks. Estuaries and Coasts, 42: 1342–1352.

Boulêtreau, S., Gaillagot, A., Carry, L., Tétard, S., De Oliveira, E., and Santoul, F. 2018. Adult Atlantic salmon have a new freshwater predator. PLoS ONE, 13: e0196046.

Brehmer, P., Do Chi, T., and Mouillot, D. 2006. Amphidromous fish school migration revealed by combining fixed sonar monitoring (horizontal beaming) with fishing data. Journal of Experimental Marine Biology and Ecology, 334: 139–150.

Burwen, D. L., Fleischman, S. J., and Miller, J. D. 2010. Accuracy and precision of salmon length estimates taken from DIDSON sonar images. Transactions of the American Fisheries Society, 139: 1306–1314.

Capoccioni, F., Leone, C., Pulcini, D., Cecchetti, M., Rossi, A., and Ciccotti, E. 2019. Fish movements and schooling behavior across the tidal channel in a Mediterranean coastal lagoon: an automated approach using acoustic imaging. Fisheries Research, 219: 105318.

Claverie, T., and Wainwright, P. C. 2014. A morphospace for reef fishes: elongation is the dominant axis of body shape evolution. PLoS ONE, 9: e112732.

Cook, D., Middlemiss, K., Jaksons, P., Davison, W., and Jerrett, A. 2019. Validation of fish length estimations from a high frequency multi-beam sonar (ARIS) and its utilisation as a field-based measurement technique. Fisheries research, 218: 59–68.

Cotter, E., and Polagye, B. 2020. Detection and classification capabilities of two multibeam sonars. In Limnology and Oceanography: Methods, 18, pp. 673–680. Wiley Online Library, Hoboken, New Jersey, United States.

Crossman, J., Martel, G., Johnson, P., and Bray, K. 2011. The use of Dual-frequency IDentification SONar (DIDSON) to document white sturgeon activity in the Columbia River, Canada. Journal of Applied Ichthyology, 27: 53–57.

Daroux, A., Martignac, F., Nevoux, M., Baglinière, J. L., Ombredane, D., and Guillard, J. 2019. Manual fish length measurement accuracy for adult river fish using an acoustic camera (DIDSON). Journal of Fish Biology, 95: 480–489.

Dunn, R. P., Kimball, M. E., O'Brien, C. G., and Adams, N. T. 2023. Characterising fish habitat use of fringing oyster reefs using acoustic imaging. In Marine and Freshwater Research, 74, pp. 139–49. CSIRO Publishing, Clayton, Australia.

Egg, L., Pander, J., Mueller, M., and Geist, J. 2018. Comparison of sonar-, camera-and net-based methods in detecting riverine fish-movement patterns. Marine and Freshwater Research, 69: 1905–1912.

Faulkner, A. V., and Maxwell, S. L. 2020. Adult Sockeye Salmon Assessment in a Tidal, Turbid River: a Comparison of Sonar and Test Fishing Methods. North American Journal of Fisheries Management, 40: 852–864.

Folpp, H., Lowry, M., Gregson, M., and Suthers, I. M. 2013. Fish assemblages on estuarine artificial reefs: natural rocky-reef mimics or discrete assemblages? PLoS ONE, 8: e63505.

Francisco, F., and Sundberg, J. 2019. Detection of visual signatures of marine mammals and fish within marine renewable energy farms using multibeam imaging sonar. Journal of Marine Science and Engineering, 7: 22.

Frias-Torres, S., and Luo, J. 2009. Using dual-frequency sonar to detect juvenile goliath grouper Epinephelus itajara in mangrove habitat. Endangered Species Research, 7: 237–242.

Froese, R., and Pauly, D. 2023. FishBase. www.fishbase.org.

Giorli, G., and Au, W. W. 2017. Application of dual frequency identification sonar for the study of deep diving odontocetes prey fields. The Journal of the Acoustical Society of America, 141: EL605–EL609.

Giorli, G., Drazen, J. C., Neuheimer, A. B., Copeland, A., and Au, W. W. 2018. Deep sea animal density and size estimated using a Dual-frequency IDentification SONar (DIDSON) offshore the island of Hawaii. Progress in Oceanography, 160: 155–166.

Gower, J. C. 1971. A general coefficient of similarity and some of its properties. Biometrics, 27: 857–871.

Grabowski, T. B., Boswell, K. M., McAdam, B. J., Wells, R. D., and Marteinsdóttir, G. 2012. Characterization of Atlantic cod spawning habitat and behavior in Icelandic coastal waters. PLoS ONE, 7: e51321.

Grote, A. B., Bailey, M. M., Zydlewski, J. D., and Hightower, J. E. 2014. Multibeam sonar (DIDSON) assessment of American shad (Alosa sapidissima) approaching a hydroelectric dam. Canadian Journal of Fisheries and Aquatic Sciences, 71: 545–558.

Grothues, T. M., Rackovan, J. L., and Able, K. W. 2016. Modification of nektonic fish distribution by piers and pile fields in an urban estuary. Journal of Experimental Marine Biology and Ecology, 485: 47–56.

Gurney, W., Brennan, L. O., Bacon, P. J., Whelan, K., O'Grady, M., Dillane, E., and McGinnity, P. 2014. Objectively assigning species and ages to salmonid length data from dual-frequency identification sonar. Transactions of the American Fisheries Society, 143: 573–585.

Harvey, E., Shortis, M., Stadler, M., and Cappo, M. 2002. A comparison of the accuracy and precision of measurements from single and stereo-video systems. Marine Technology Society Journal, 36: 38–49.

Helminen, J., Dauphin, G. J., and Linnansaari, T. 2020. Length measurement accuracy of adaptive resolution imaging sonar and a predictive model to assess adult Atlantic salmon (Salmo salar) into two size categories with long-range data in a river. Journal of fish biology, 97: 1009–1026.

Helminen, J., and Linnansaari, T. 2021. Object and behavior differentiation for improved automated counts of migrating river fish using imaging sonar data. Fisheries Research, 237: 105883.

Hightower, J. E., Magowan, K. J., Brown, L. M., and Fox, D. A. 2013. Reliability of fish size estimates obtained from multibeam imaging sonar. Journal of Fish and Wildlife Management, 4: 86–96.

Holmes, J. A., Cronkite, G., and Enzenhofer, H. J. 2005. Salmon enumeration in the Fraser River with the dual-frequency identification sonar (DIDSON) acoustic imaging system. The Journal of the Acoustical Society of America, 117: 2367–2368.

Hughes, J. B., and Hightower, J. E. 2015. Combining split-beam and dual-frequency identification sonars to estimate abundance of anadromous fishes in the Roanoke River, North Carolina. North American Journal of Fisheries Management, 35: 229–240.

Jing, D., Han, J., and Zhang, J. 2018. A method to track targets in three-dimensional space using an imaging sonar. Sensors, 18: 1992

Jones, R. E., Griffin, R. A., and Unsworth, R. K. 2021. Adaptive Resolution Imaging Sonar (ARIS) as a tool for marine fish identification. Fisheries Research, 243: 106092.

Jůza, T., Rakowitz, G., Draštík, V., Blabolil, P., Herzig, A., Kratochvíl, M., Muška, M *et al.* 2013. Avoidance reactions of fish in the trawl mouth opening in a shallow and turbid lake at night. Fisheries research, 147: 154–160.

Kaufman, L., and Rousseeuw, P. J. 2009. Finding groups in data: an introduction to cluster analysis. John Wiley & Sons, Hoboken, New Jersey, United States.

Keefer, M. L., Caudill, C. C., Johnson, E. L., Clabough, T. S., Boggs, C. T., Johnson, P. N., and Nagy, W. T. 2017. Inter-observer bias in fish classification and enumeration using dual-frequency identification sonar (didson): a pacific lamprey case study. Northwest Science, 91: 41–53.

Kerschbaumer, P., Tritthart, M., and Keckeis, H. 2020. Abundance, distribution, and habitat use of fishes in a large river (Danube, Austria): mobile, horizontal hydroacoustic surveys vs. a standard fishing method. ICES Journal of Marine Science, 77: 1966–1978.

Kimball, M. E., Rozas, L. P., Boswell, K. M., and Cowan Jr, J. H. 2010. Evaluating the effect of slot size and environmental variables on the passage of estuarine nekton through a water control structure. Journal of Experimental Marine Biology and Ecology, 395: 181–190.

Lagarde, R., Peyre, J., Amilhat, E., Mercader, M., Prellwitz, F., Simon, G., and Faliex, E. 2020. In situ evaluation of European eel counts and length estimates accuracy from an acoustic camera (ARIS). In Knowledge & Management of Aquatic Ecosystems, 44. EDP Sciences, Les Ulis, France.

Lagudi, A., Bianco, G., Muzzupappa, M., and Bruno, F. 2016. An alignment method for the integration of underwater 3D data captured by a stereovision system and an acoustic camera. Sensors, 16: 536.

Langkau, M., Balk, H., Schmidt, M., and Borcherding, J. 2012. Can acoustic shadows identify fish species? A novel application of imaging sonar data. Fisheries Management and Ecology, 19: 313–322.

Lankowicz, K. M., Bi, H., Liang, D., and Fan, C. 2020. Sonar imaging surveys fill data gaps in forage fish populations in shallow estuarine tributaries. Fisheries Research, 226: 105520.

Lawrence, J., and Fernandes, P. G. 2022. A typology of North Sea oil and gas platforms. Scientific Reports, 12: 1–7.

Lin, D., Zhang, H., Kang, M., and Wei, Q. 2016. Measuring fish length and assessing behaviour in a high-biodiversity reach of the Upper Yangtze River using an acoustic camera and echo sounder. Journal of Applied Ichthyology, 32: 1072–1079.

Madgett, A. S., Harvey, E. S., Driessen, D., Schramm, K. D., Fullwood, L. A., Songploy, S., Kettratad, J *et al.* 2022. Spawning aggregation of bigeye trevally, Caranx sexfasciatus, highlights the ecological importance of oil and gas platforms. Estuarine, Coastal and Shelf Science, 276: 108024.

Maechler, M., Rousseeuw, P., Struyf, A., Hubert, M., and Hornik, K. 2012. Cluster: cluster analysis basics and extensions. R package version, 1: 56.

Magowan, K., Reitsma, J., and Murphy, D. 2012. Use of dual-frequency identification sonar to monitor adult river herring in a small coastal stream. Marine and Coastal Fisheries, 4: 651–659.

Martignac, F., Daroux, A., Bagliniere, J., Ombredane, D., and Guillard, J. 2015. The use of acoustic cameras in shallow waters: new hydroacoustic tools for monitoring migratory fish population. Fish and Fisheries, 16: 486–510.

McCauley, D. J., DeSalles, P. A., Young, H. S., Papastamatiou, Y. P., Caselle, J. E., Deakos, M. H., Gardner, J *et al.* 2014. Reliance of mobile species on sensitive habitats: a case study of manta rays (Manta alfredi) and lagoons. Marine biology, 161: 1987–1998.

McClatchie, S., Thorne, R. E., Grimes, P., and Hanchet, S. 2000. Ground truth and target identification for fisheries acoustics. Fisheries Research, 47: 173–191.

McLean, D., Vaughan, B., Malseed, B., and Taylor, M. 2020. Fish-habitat associations on a subsea pipeline within an Australian Marine Park. Marine environmental research, 153: 104813.

Miki, T., Nakatsukasa, H., Takahashi, N., Murata, O., and Ishibashi, Y. 2011. Aggressive behaviour and cannibalism in greater amberjack, Seriola dumerili: effects of stocking density, feeding conditions and size differences. Aquaculture Research, 42: 1339–1349.

Moursund, R. A., Carlson, T. J., and Peters, R. D. 2003. A fisheries application of a dual-frequency identification sonar acoustic camera. ICES Journal of Marine Science, 60: 678–683.

Mueller, R. P., Brown, R. S., Hop, H., and Moulton, L. 2006. Video and acoustic camera techniques for studying fish under ice: a review and comparison. Reviews in Fish Biology and Fisheries, 16: 213–226.

Parsons, M. J., Fenny, E., Lucke, K., Osterrieder, S., Jenkins, G., Saunders, B. J., Jepp, P *et al.* 2017. Imaging marine fauna with a Tritech Gemini 720i sonar. Acoustics Australia, 45: 41–49.

Parsons, M. J., Parnum, I. M., Allen, K., McCauley, R. D., and Erbe, C. 2014. Detection of sharks with the Gemini imaging sonar. Acoust. Aust, 42: 185–190.

Pipal, K. A., Notch, J. J., Hayes, S. A., and Adams, P. B. 2012. Estimating escapement for a low-abundance steelhead population using dual-frequency identification sonar (DIDSON). North American Journal of Fisheries Management, 32: 880–893.

Pitcher, T. 2001. Fish schooling. Encyclopedia of ocean sciences: marine biology, 337–349.

Rakowitz, G., Tušer, M., Říha, M., Jůza, T., Balk, H., and Kubečka, J. 2012. Use of high-frequency imaging sonar (DIDSON) to observe fish behaviour towards a surface trawl. Fisheries Research, 123–124: 37–48.

Rieucau, G., Boswell, K. M., Kimball, M. E., Diaz, G., and Allen, D. M. 2015. Tidal and diel variations in abundance and schooling behavior of estuarine fish within an intertidal salt marsh pool. Hydrobiologia, 753: 149–162.

Rose, C. S., Stoner, A. W., and Matteson, K. 2005. Use of high-frequency imaging sonar to observe fish behaviour near baited fishing gears. Fisheries research, 76: 291–304.

Shahrestani, S., Bi, H., Lyubchich, V., and Boswell, K. M. 2017. Detecting a nearshore fish parade using the adaptive resolution imaging sonar (ARIS): an automated procedure for data analysis. Fisheries Research, 191: 190–199.

Sibley, E. C., Madgett, A. S., Elsdon, T. S., Marnane, M. J., Harvey, E. S., and Fernandes, P. G. 2023a. The capacity of imaging sonar for quantifying the abundance, species richness, and size of reef fish assemblages. Marine Ecology Progress Series, 717: 157–179.

Sibley, E. C., Elsdon, T. S., Marnane, M. J., Madgett, A. S., Harvey, E. S., Cornulier, T., Driessen, D *et al*. 2023b. Sound sees more: a comparison of imaging sonars and optical cameras for estimating fish densities at artificial reefs. Fisheries Research, 264: 106720.

Simmonds, E., and MacLennan, D. 2005. Fisheries acoustics. In Theory and Practice, 2nd edn. Blackwell Science, Oxford, United Kingdom.

Stanton, T. K., Chu, D., Jech, J. M., and Irish, J. D. 2010. New broadband methods for resonance classification and high-resolution imagery of fish with swimbladders using a modified commercial broadband echosounder. ICES Journal of Marine Science, 67: 365–378.

Team, R. C. 2013. R: A language and environment for statistical computing. R Foundation for Statistical Computing, Vienna, Austria. http://www. R-project.org/.

Tušer, M., Frouzová, J., Balk, H., Muška, M., Mrkvička, T., and Kubečka, J. 2014. Evaluation of potential bias in observing fish with a DIDSON acoustic camera. Fisheries Research, 155: 114–121.

Van Hal, R., Griffioen, A., and Van Keeken, O. 2017. Changes in fish communities on a small spatial scale, an effect of increased habitat complexity by an offshore wind farm. Marine Environmental Research, 126: 26–36.

Viehman, H. A., and Zydlewski, G. B. 2015. Fish interactions with a commercial-scale tidal energy device in the natural environment. Estuaries and Coasts, 38: 241–252.

Viscido, S. V., Parrish, J. K., and Grünbaum, D. 2004. Individual behavior and emergent properties of fish schools: a comparison of observation and theory. Marine Ecology Progress Series, 273: 239–249.

Viscido, S. V., Parrish, J. K., and Grünbaum, D. 2007. Factors influencing the structure and maintenance of fish schools. Ecological modelling, 206: 153–165.

Wei, Y., Duan, Y., and An, D. 2022. Monitoring fish using imaging sonar: capacity, challenges and future perspective. In Fish and Fisheries. Wiley Online Library, Hoboken, New Jersey, United States.

Wetz, J. J., Ajemian, M. J., Shipley, B., and Stunz, G. W. 2020. An assessment of two visual survey methods for documenting fish community structure on artificial platform reefs in the Gulf of Mexico. Fisheries Research, 225: 105492.

Zhang, H., Wei, Q., and Kang, M. 2014. Measurement of swimming pattern and body length of cultured Chinese sturgeon by use of imaging sonar. Aquaculture, 434: 184–187.

Handling editor: David Demer

Received: 26 May 2023; **Revised:** 18 August 2023; **Accepted:** 20 September 2023